Nuclear code case development of printed-circuit heat exchangers with thermal and mechanical performance testing

Shaun R. Aakre
Graduate Research Assistant
University of Wisconsin
Madison, WI

Ian W. Jentz
Graduate Research Assistant
University of Wisconsin
Madison, WI

Mark H. Anderson
Research Professor
University of Wisconsin
Madison, WI

Shaun Aakre is a graduate research assistant working for Dr. Mark Anderson. His research involves testing compact heat exchangers using multiple coolants (sodium, salt, supercritical CO_2) and performing non-destructive evaluations and destructive tests on these units. He completed his B.S. in nuclear engineering in May 2017 and is now working toward a M.S. in mechanical engineering with a certificate in strategic innovation.

Ian Jentz is a research assistant in Dr. Anderson's group. His research investigates both thermal performance and mechanical integrity of printed circuit heat exchangers. His focus is on modeling, and experimental measurement of, thermal shock and transients with sCO_2 recuperators. He completed his M.S. in nuclear engineering in December of 2016 and is currently working toward his Ph.D.

Dr. Mark Anderson is a research professor in the Department of Engineering Physics and Director of the Thermal Hydraulic Laboratory at the University of Wisconsin– Madison. He also manages the UW – Madison Tantalus facility in Stoughton, WI. Dr. Anderson studies the physics, thermal hydraulic performance and material corrosion issues of several fluids (salts, liquid metals, supercritical water and carbon dioxide).

ABSTRACT

The U.S. Department of Energy has agreed to fund a three-year integrated research project to close technical gaps involved with compact heat exchangers to be used in nuclear applications. This paper introduces the goals of the project, the research institutions, and industrial partners working in collaboration to develop a draft Boiler and Pressure Vessel Code Case for this technology. Heat exchanger testing, as well as non-destructive and destructive evaluation, will be performed by researchers across the country to understand the performance of compact heat exchangers. Testing will be performed using coolants and conditions proposed for Gen IV Reactor designs. Preliminary observations of the mechanical failure mechanisms of the heat exchangers using destructive and non-destructive methods is presented. Unit-cell finite element models assembled to help predict the mechanical behavior of these high-temperature components are discussed as well. Performance testing methodology is laid out in this paper along with preliminary modeling results, an introduction to x-ray and neutron inspection techniques, and results from a recent pressurization test of a printed-circuit heat exchanger. The operational and quality assurance knowledge gained from these models and validation tests will be useful to developers of supercritical CO_2 systems, which commonly employ printed-circuit heat exchangers.

INTRODUCTION

While compact heat exchangers have become a relatively mature technology, their implementation into the nuclear industry has just begun. Until now, no attempt has been made to codify a compact heat exchangers for Section III of the American Society of Mechanical Engineers (ASME) Boiler and Pressure Vessel Code (BPVC), which deals with construction of nuclear-grade equipment. Historical focus on light-water reactors (LWR) has developed shell and tube heat exchangers (STHE) for nuclear applications. These are well-understood and relatively easy to inspect for cracks and leaks using established non-destructive evaluation techniques. In next generation reactors the traditional STHE may not be the optimal selection as its mechanical strength is limited and its cost when advanced alloys are used becomes prohibitive. Compact heat exchangers (CHE) utilizing high surface area to volume ratios (greater than 200 m^2/m^3) optimize thermal effectiveness and cost, especially when the use of expensive super-alloys is considered. There are multiple types of CHE available (fin-tube, plate-type, plate-fin, and micro-tube). The printed-circuit heat exchanger (PCHE) is investigated by this project because it offers the ability to contain the high pressures of gas and supercritical coolants at the high operating temperatures associated with liquid metals and molten salts.

The PCHE is created by "printing" flow channels into thin plates of stainless steel or nickel-alloys using a chemical etchant. Several of these plates are then stacked so the plates alternate between the hot and cold fluid streams, as shown in Figure 1. This stack is then compressed in a vacuum furnace at high temperature to fuse the plates together through a diffusion bonding process. Headers and pipe stand-offs are then welded to the diffusion-bonded block.
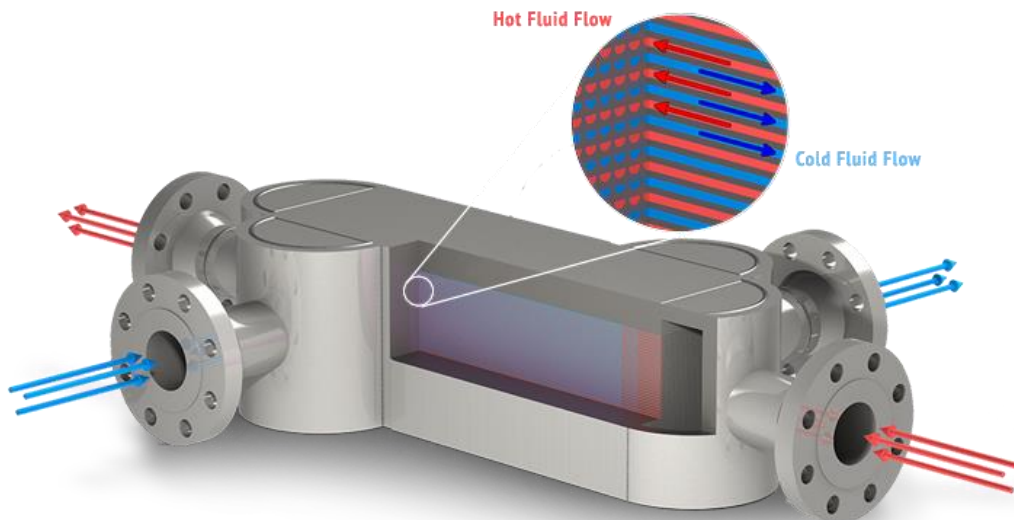
Fig. 1. Cutaway image of straight-channel PCHE with headers and flanges attached.

IMPLICATIONS FOR NUCLEAR INDUSTRY

Advanced or Generation IV nuclear reactors encompass six design concepts which use either molten salt, liquid sodium or lead, supercritical water (SCW), or helium as primary coolants [1]. All six concepts have been determined to be viable for near-term deployment. A common goal of these designs is to push the reactor core outlet temperature from the ~300°C maximum for LWRs, to between 500-850°C for enhanced efficiency. To achieve this goal, the best high-temperature equipment (pumps, valves, heat exchangers, and piping) need to be selected and BPVC certified. The primary heat exchanger is perhaps the largest, most expensive, and most crucial component to these high temperature, high pressure systems. To begin the optimization and licensing of these components for nuclear applications, the U.S. DoE has funded an investigation of printed-circuit heat exchanger's thermal and mechanical performance.

High surface area to volume ratio of CHEs provides performance improvements and potential cost-reductions that could have a significant impact on the economics of advanced nuclear power plants. These heat exchangers are used in the economical supercritical carbon dioxide (sCO_2) power cycle. This cycle enables higher operating temperatures than existing modified-Rankine cycles, thus achieving higher thermal efficiencies. Unfortunately, the high working pressure and temperature of sCO_2 prevents STHEs from being a practical option, especially if load-following capabilities are desired [2]. PCHEs have been used in prototypic high-temperature sCO_2 systems for nearly two decades. Over this period, the sCO_2 cycle has shown great promise for high temperature power plants while eliminating many issues involved with sub- and supercritical steam. Although there is less industrial evidence to support it, developers also believe a commercial scale sCO_2 Brayton cycle's relative simplicity to modified-Rankine systems will have additional capital and maintenance cost reductions. For these reasons, nuclear certification of the PCHE would be a huge breakthrough for both supercritical CO_2 power cycles and advanced nuclear systems.

DEVELOPMENT METHODOLOGY

The goal of the three-year U.S. Department of Energy Integrated Research Project (IRP) is to advance understanding of the performance, integrity and lifetime of PCHEs in nuclear power applications. These advancements will be organized into a draft Section III code case for printed-circuit heat exchangers along with a list of remaining technical gaps. The project is divided into five focus groups: code case development, mechanical strength investigation, prototypic heat exchanger testing, non-destructive, and destructive evaluation. These tasks have been integrated into a feedback loop, shown in Figure 2, between the code case developers and the testing bodies.
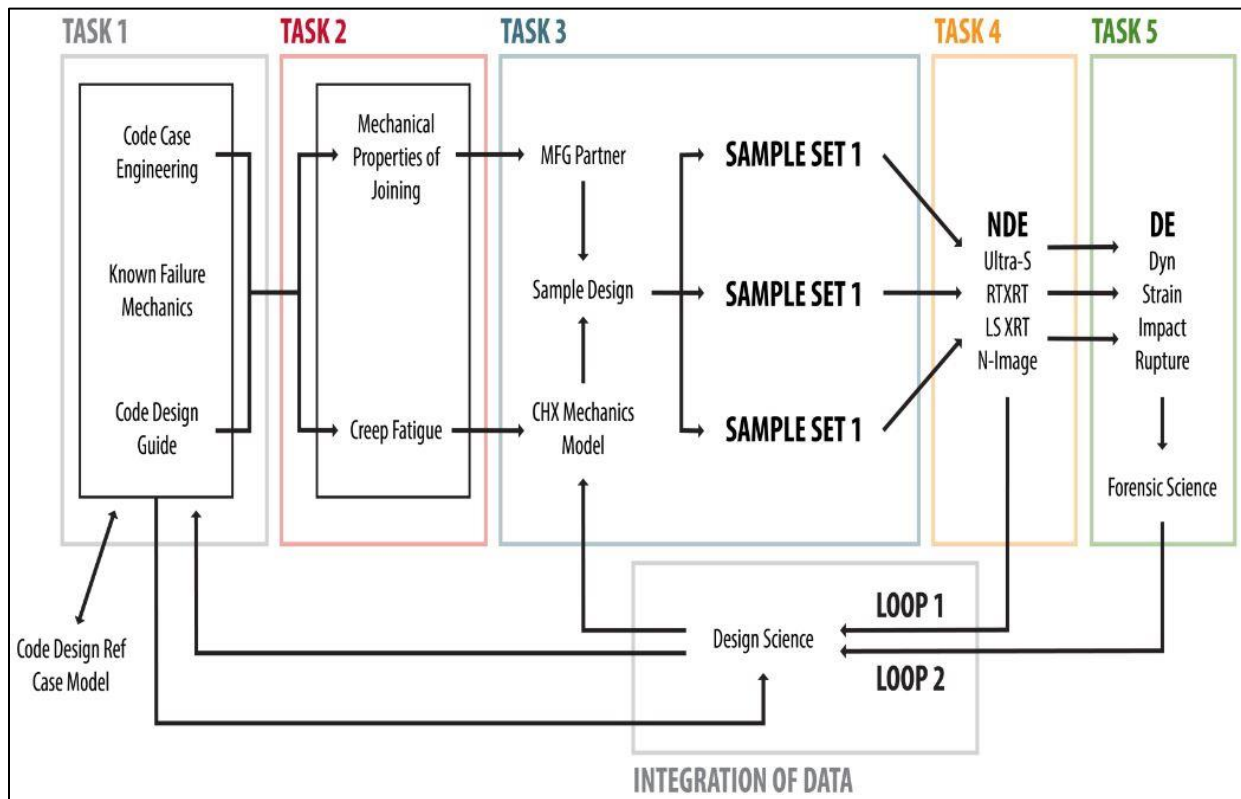
Fig. 2. Research Project Task Flow

Task 1 will be led by MPR Associates, a technical firm which provides consultation on a wide variety of energy systems and BPVC case development. Their expertise will focus the research effort on gaps in the existing code that need to be addressed in order to make meaningful progress towards near-term certification. The draft code case assembled by MPR will identify technical gaps that will be investigated by Tasks 2-5. Once initial tests have been performed, processed data will be reviewed by MPR and determined to be within the bounds of existing code sections. If additional information is required this will be relayed to the other task groups for further testing and evaluation.

North Carolina State University (NCSU) leads Task 2, which measures material strength properties of diffusion-bonded cores and performs finite element analyses using this data. Bonded samples with and without etched micro-channels are cut into tensile "dog-bone" specimens for tensile and creep strength testing. By cutting samples at different orientations from the PCHE core, the strength of the PCHE can be measured parallel to the flow direction, across the flow direction, or through the plate stack. This allows researchers to obtain macroscopic orthotropic material properties for finite element analyses. These tests will also determine if the diffusion bonds have similar strength to the base nuclear-grade materials to be used. If this is true, PCHE cores do not have to be de-rated to account for an inherent weakness due to the bond.

The University of Wisconsin leads tasks 3 and 5, which deal with PCHE performance testing and destructive analysis. These are discussed in greater detail in the following sections. The Electric Power Research Institute (EPRI) will be in charge of task 4 which focuses on non-destructive evaluation (NDE). EPRI has extensive experience with industrial ultrasonic imaging and weld inspection techniques. Use of these techniques in the existing nuclear fleet provides precedent for their application in CHE inspection. As discussed in the NDE section, CHEs present significant challenges to traditional inspection methods because of their density and the reduced size of troublesome artifacts. A discussion of UW's initial investigation of radiography inspection techniques has been included in the following sections as well.

To decrease the cycle time of the feedback loop in Figure 2, the scope of tasks 2-5 was limited early in the project. The printed-circuit heat exchanger was the CHE chosen for this project because of its applicability to supercritical-fluid and gas cooled systems and its ability to operate at higher temperatures than other CHE. Additionally, there are only five alloys codified for Class 1 components of nuclear systems (components whose failure would lead to consequences of 'high' severity). Recent research and industry interests have identified the sodium or lead fast reactor and molten salt reactor as the three Gen IV designs closest to commercial deployment [1]. In an attempt to direct this work towards near-term advanced nuclear systems, Incoloy 800H and stainless steel 316H were the two alloys chosen for this project because of interest of Gen IV developers in these alloys.

Furthermore, there are numerous PCHE geometries that have excellent thermal effectiveness and a low pressure drop. The herringbone and the ShimRex© geometries shown in Figures 3 and 4, respectively, were chosen because of extensive fabrication experience and exceptional thermal performance. These geometries will be etched and bonded by two industry collaborators, Vacuum Process Engineers (VPE) and CompRex. VPE has extensive experience in diffusion bonding techniques and will be etching the herringbone geometries and bonding all PCHE for this project. CompRex is a Wisconsin-based company which specializes in high-performance PCHEs for chemical reaction and heat exchange applications. The ShimRex® geometry is one of their proprietary designs which uses plates that are etched completely through to form the elongated slots seen in Figure 4. The slots of the adjacent plate are slightly offset so the material left between the slots forms a small flow obstruction or "fin" which significantly improves heat transfer. The University of Wisconsin has extensively investigated the 'airfoil' geometry which is discussed in further detail in the mechanical modeling section below. While the modeling techniques established by investigating this geometry have been valuable, the discontinuous nature of the airfoil geometry was determined to be more difficult to code-qualify compared to the geometries shown below.
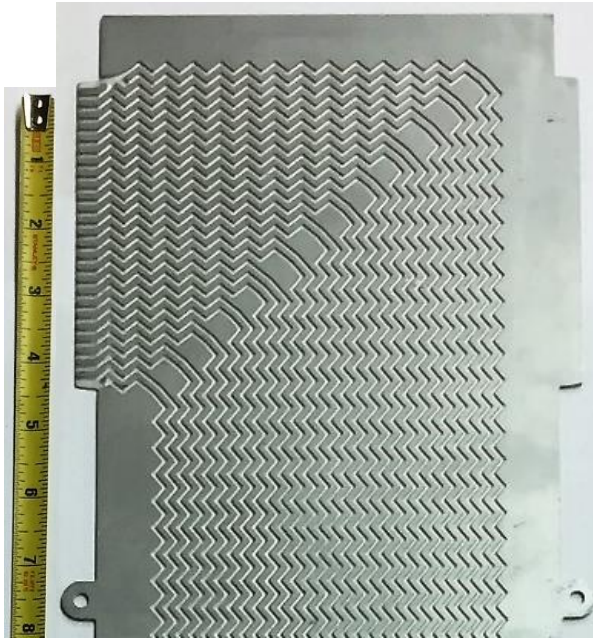
Fig. 3. Herringbone or "zig-zag" geometry   **Fig. 4.** ShimRex® geometry
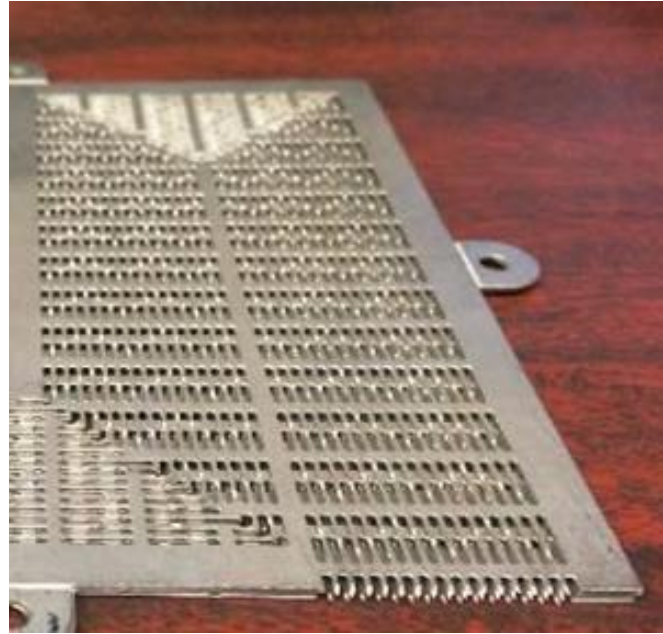
TESTING OF PROTOTYPIC PCHE

Distribution of test units and conditions

Printed circuit heat exchangers have been tested by universities and laboratories across the US for over two decades now. Multiple testing facilities are available to test PCHEs with a variety of coolants. The testing matrix in Table 1 shows the universities involved with prototypic PCHE testing (Task 3) and the coolants they will be testing in the first year of the project.

Table 1. PCHE coolant configurations to be tested in Year 1

University	Hot Side (primary coolant)	Max. Hot Temp.	Cold Side (working fluid)
Georgia Institute of Technology	Helium	650°C	sCO_2
University of Idaho	sCO2	600°C	sCO_2
	Helium	600°C	Helium
University of Michigan – Ann Arbor	Helium	850°C	FLiNaK salt
	FLiNaK salt	700°C	sCO_2
University of Wisconsin – Madison	Sodium	700°C	sCO_2
	NaNO3 – KNO3 salt	600°C	Air

Each coolant combination is one that could be expected in a Generation IV nuclear plant, except the sCO_2 to sCO_2 and sodium/potassium nitrate salt to air. The first of these will be tested by the University of Idaho for long periods of steady-state operation. Channel clogging and cleaning techniques will be thoroughly investigated during these tests. In 2014, Kruizenga concluded fouling issues in PCHE used on Sandia's recompression CO_2 Brayton cycle were due to a combination of dirt, metallic corrosion products, and residual hydrocarbons which may have been introduced by lower purity CO_2 (99.9% vs. 99.95%) used during previous experiments [3]. The tests done at Idaho with sCO_2 and helium will attempt to quantify these fouling mechanisms and identify how to remove deposits using cleansing solvents and "puffing" techniques. The second coolant combination which utilizes a nitrate salt is chosen purely because of operational simplicity over fluorides. The University of Wisconsin has a high capacity nitrate salt loop which can accommodate this PCHE test with almost no modification. The sodium nitrate and potassium nitrate salt mixture melts around 220°C versus 455°C for FLiNaK, a fluoride salt. Thus a nitrate salt will allow for a wider operating temperature range using a proven experimental setup to obtain information related to the

use of molten salts in PCHEs. As an aside, the nitrate salt to air configuration data will be valuable to the concentrating solar power (CSP) industry, which uses the same or similar nitrate salt mixtures as a collector fluid or thermal storage medium. Since sCO_2 is also being investigated for CSP, knowledge about the behavior of nitrate salts and sCO_2 in PCHE will also be of great value to next generation solar plants.

In the planning stages, there was significant overlap between the testing capabilities of each institution. The six coolant combinations shown in Table 1 were assigned based on availability of experimental facilities and the temperature, pressure and flow capabilities of these facilities. Previous experience at UW-Madison led the authors to choose a PCHE designed to transfer 15 kW of heat. These units will be approximately the size shown in Figure 5. To reduce fabrication costs, some coolant combinations will use the same internal geometry as another. It is common practice to diffusion bond up to 3 small PCHE at once from a single plate stack and cut the stack into the individual PCHE after bonding is complete. Since these PCHE will be used for different coolants, the internal geometry may not be optimal from a thermal performance standpoint for a given fluid. However, this is acceptable because the purpose of this project is not to optimize the design for each coolant, but to identify areas of concern as related to mechanical failure. Until now, no PCHE has been tested with sodium or a molten salt (fluoride or nitrate) and minimal investigation has been done with air. The data collected from these tests will flag any code qualification hurdles and be extremely valuable to designers of prototype advanced reactor systems.

Fig. 5. Prototypic PCHE with internal capillary tubes (seen on right end).

Instrumentation

PCHE instrumentation has made significant progress in the last two decades. The most common instruments used to evaluate the performance of these systems are pressure transducers (absolute and differential), thermocouples, and mass flow meters. In the last five years, fiber optics have received a high amount of attention from thermal researchers, because of their temperature and strain sensing capabilities. When optical fibers made from silica or gallium arsenide are stretched or heated they produce a phase shift in a localized area. Therefore, light pulses sent down the fiber by a controller are reflected back at a different frequencies than the original pulse. Using the known properties of the fiber, the measured phase shifts, and response time of the reflected light, the controller can determine the temperature or strain with exceptional accuracy and a spatial resolution of less than 2.5 millimeters [4]. Also the time-resolution of these fibers ranges between 20 and 250 Hz, allowing rapid transient test to be performed.

When evaluating the thermal performance of PCHE geometries, is it important to know temperatures within the heat exchanger in addition to the four terminal temperatures. The University of Wisconsin has made the PCHEs containing 8 stainless steel capillary tubes embedded in the diffusion-bonded core between a set hot and cold fluid passages (see Fig. 5). These capillaries can be seen on the right-end of the PCHE block. Optical fibers are inserted into these capillaries to obtain a continuous axial temperature profiles along 8 parallel lines. Using a MATLAB code, these profiles can be interpolated to obtain a 2-D temperature contour like the one shown in Figure 6.
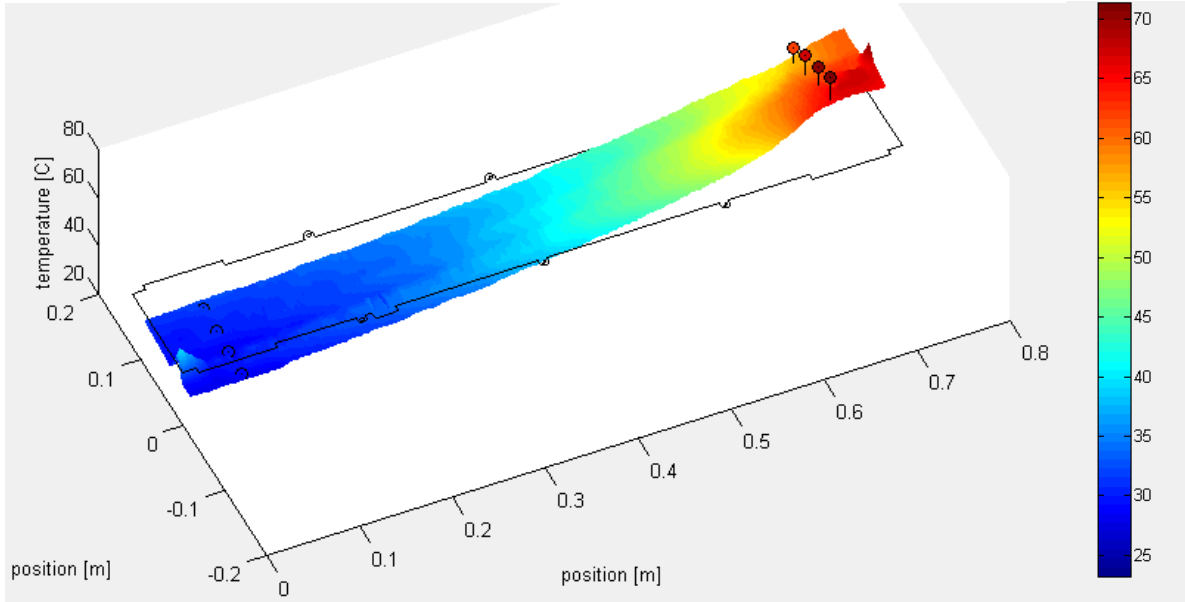
Fig. 6. Interpolated temperature profile of plate separating hot and cold streams

Temperature profiles like the one in Figure 6 can be used to estimate thermal stresses within the PCHE during transient tests. However, since this work will attempt to quantify mechanical as well as thermal performance, fiber optics are also being investigated as a method of strain measurement during transient tests. The major difference between temperature and strain sensing fibers is the latter must be secured to the surface of the heat exchanger using a special adhesive. This is particularly challenging because of the discrepancy between the thermal expansion of the PCHE material and the fiber/adhesive. In 2016, sapphire fibers were used to measure 10 *μ-strain* increments at 600°C and higher temperature operation is assumed possible [7]. Traditional strain gauges are being investigated as well, but similar issues exist with high temperature operation. It is likely several types of strain instrumentation will be incorporated into the test units to increase the chances of getting good transient strain data. The location of strain sensors will be finalized pending results of FEA transient simulations which will identify areas of interest. The first set of PCHEs will closely resemble the unit in Figure 5, with strain transducers embedded on the same plates containing the capillary tubes to reduce material and fabrication costs. Additionally, each test stand will have a Coriolis or Venturi mass flow mater, terminal temperature thermocouples, and differential pressure transducers for each stream. Using this collection of instruments, performance maps can be created over a range of conditions with a variety of coolants as discussed in the following section.

Steady-State Testing Methodology

Once the PCHEs are fabricated by the industry collaborators (CompRex and VPE), each institution will perform a series of steady-state and transient tests. The method of performing steady-state tests at the University of Wisconsin is summarized here. Once proper operation of instrumentation and equipment has been confirmed, the mass flow rates of each coolant can be manipulated to collect flow and heat transfer correlation data. For example, using the measured pressure drop and mass flow rate with a density determined from temperature and pressure readings, Darcy's friction factor can be determined using Eq. 1. As the mass flow rate and system pressure are changed, a performance map can be constructed by plotting friction factor versus Reynolds number, which is calculated using Eq. 2.

$$\Delta P = f \frac{L}{D_h} \frac{1}{2} \rho v^2 \qquad \textbf{[1]}$$

$$Re = \frac{\rho v D_h}{\mu} = \frac{\dot{m} D_h}{A_C \mu} \qquad \textbf{[2]}$$

Heat transfer performance of the PCHE can be measured using the terminal temperatures and capacitance rates, using the overall UA method which is commonly employed in STHE sizing. To obtain a more precise performance metric, the temperatures measured by the fiber optic sensors discussed above

can be used with a constant volume approach to discretize the PCHE. This method accounts for spatial variations of the heat transfer coefficient due to CO_2 property variation. The dimensionless Colburn factor can be calculated using a local heat transfer coefficient "h" or the overall coefficient "U" as seen in Eq. 3. The first of these allows the analyst to plot Colburn factor, "j", as a function of position in the PCHE, while the latter can be plotted versus Reynolds number as a heat transfer performance map for a given geometry [5].

$$j = \frac{h \, Pr^{2/3} A_C}{C_p \, \dot{m}} = \frac{(UA)A_C}{A_S} \frac{Pr^{2/3}}{C_p \, \dot{m}} \qquad \textbf{[3]}$$

Running a series of steady-state tests will allow each operator to determine the operational limits of their experiment and confirm all instrumentation is working as expected. Once operation of the experiment is deemed satisfactory, the operator can move onto transient testing. The variety of coolants to be used in Task 3 provides a challenge for transient testing, because the relevance of each transient test to a postulated nuclear designs is heavily-dependent on the coolant. Therefore, each institution will need to define the abilities of their systems and select their transient tests accordingly.

Transient Testing Goals

To obtain the most useful data from these transient tests as possible, a list of Code Case gaps and commercialization gaps have been complied. This list includes questions about the creep, fatigue and ratcheting behavior of PCHE for code qualification, in addition to questions about acceptable thermal ramp rate and methods to identify and mitigate fouling in commercial-scale units. To answer these questions, an individual test has been assigned to the task of quantifying each phenomenon. For example, the University of Wisconsin will attempt to observe accelerated creep behavior by designing a PCHE with especially thin inter-channel walls. This unit will be tested under high pressure (~25MPa) and high temperature (>600°C) for a minimum of 500 hours. Another test will strive to thermally ratchet a PCHE by subjecting the unit to many successive temperature oscillations. Yet another test will subject the PCHE to rapid thermal ramps to validate FEA models and predict safe operating limits for potential users. UW will focus on the ShimRex® geometry while University of Michigan and the Georgia Institute of Technology will be performing similar transient tests on the herringbone designs. Clogging issues will be studied in parallel with the transient tests and as the primary concern of University of Idaho's long-term steady state tests.

The resulting transient response data will be essential to modeling PCHE performance during anticipated operational occurrences (AOO) such as plant start-up, shut-down, aggressive load following, and pump trips, in addition to design-basis events (DBE) such as simulated reactivity insertions and protected loss of heat sink. Ideally, transient tests will increase in severity until the test stand as reached its limits or the PCHE fails due to thermally-induced stresses. The temperature and strain data collected during these tests will be organized and used to construct and validate FEA models built by NCSU and UW-Madison mechanics experts. Failed and/or stressed units will be compared to untested PCHE with the same internal structure using the NDE and DE methods discussed in the following sections.

Wisconsin Testing Facilities

The University of Wisconsin has been testing PCHEs with supercritical CO_2 for over 12 years. Over this time, testing facilities have been updated to increase operating temperatures and pressures and to introduce new instrumentation such as embedded thermocouples and optical fibers. In Table 1, one can see the coolant combinations to be tested at the University of Wisconsin are sodium to sCO_2 and salt to air. A reciprocating CO_2 pump capable of 13.5 GPM at 4350psi is currently being integrated into a flow loop which will extract heat from an operational sodium loop, shown in Figure 7. This loop uses a moving magnet pump which pushes liquid sodium through a rectangular conduit using only the Lorentz generated by the motion of the magnets outside the conduit. This pump can produce flow rates of up to 40 GPM, which is more than ten times the flow rate required for the steady-state tests. A special transient heater using three 6-kW cartridge heaters will be used for rapid temperature transients on the sodium side of the PCHE.

Fig. 7. UW Sodium Loop

Fig. 8. UW Nitrate Salt Loop

A second testing configuration will use air to extract heat from the high-capacity nitrate salt loop shown in Figure 8. This salt loop is capable of flows up to 160 GPM and has a maximum operating temperature of 600°C. Twin roots-type blowers designed by UW to cool large brazed-plate heat exchangers will supply the air flow. Both the salt loop and air supply are significantly oversized for the 15 kW PCHE, so a wide range of temperatures and flow rates can be achieved. While nitrate salts are not considered as a primary coolant in nuclear reactors, it is much simpler to use because of its lower melting point compared to fluorides. Additionally, high temperature salt-to-air heat exchangers are required for conceptual combined cycles nuclear plants, such Berkeley's molten salt pebble-bed reactors which hopes to make use of natural gas peaking. The data collected from this configuration will also be extremely valuable to concentrating solar power plants, which may use PCHEs to transfer heat from sCO_2 or superheated steam to the thermal storage medium, nitrate salt. Both experiments will be monitored and controlled by LabVIEW programs which will allow operating parameters to be easily adjusted and recorded for each test.

MECHANICAL INTEGRITY MODELING

To supplement experimental data obtained from steady-state and transient tests, finite element models are being created to simulate the expected results that can be compared with experimental observations. Models have been developed to consider the complexities of the geometry and the time-dependent behavior of the material, such as creep and ratcheting. These models are developed starting from the simplest geometries with the most basic material properties and stress model assumptions and progressively built-up to include additional complexities once proper solutions are confirmed. The methodology and some results from examination of the 'airfoil' geometry, shown in Figure 9, are summarized here. This methodology is similar to the current work being performed at Wisconsin on the zig-zag and ShimRex geometries for the nuclear code case development project. One important distinction to be made is that the following modeling work assumes SS316L material properties. All physical PCHEs studied up to the present work were constructed of this alloy because of relatively low cost and ease of the diffusion bonding process.

Mechanically, the airfoil-fin PCHE presents a unique problem in the evaluation of its strength. Unlike straight and zig-zag PCHE designs which use some form of continuous walled micro-channels, the airfoil-fin design has discontinuous supports between plates. This support pattern creates unique three-dimensional stress distributions which requires three-dimensional analysis. There is a great deal more complexity than is present in the stress distributions of straight and zig-zag micro-channels, which are generally two dimensional. Additional complexity results from the consideration of the entirety of a heat exchanger, including supporting exterior walls and manifolding structures.
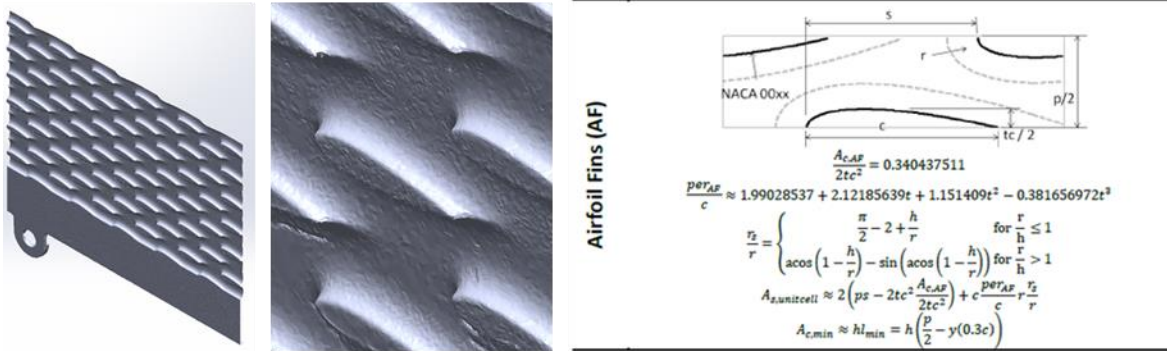
Fig. 9. (left) optical scan of airfoil-fin channel, (center) optical scan detail, (right) camber-less NACA airfoil equation and airfoil-fin pattern [8]

Table 2. Airfoil Geometry Dimensions

Description	Symbol	Unit	Design Value
Chord length	c	mm	8.1
Thickness	tc	mm	0.2
Axial pitch	s	mm	6.9
Lateral pitch	p	mm	7.3
Fillet radius	r	mm	0.95
Channel depth	d	mm	0.95
Hydraulic Diameter	D_h	mm	1.607

Fabrication and Diffusion-Bonding Considerations

Integrity of the diffusion bond is especially important in the airfoil fin PCHE because stress concentrating features coincide with the diffusion bond interface. As such the fabrication of the PCHEs is just as important as channel geometry and design loading. Recall, during the diffusion bonding process the plates are placed under load at elevated temperatures within an inert atmosphere or vacuum. This is accomplished in specialized vacuum furnaces. Loads are less than the yield strength of the parent material and temperatures are typically 50-80% that of the material melting point. Duration of loading and heating are varied to achieve the strongest bond for a particular geometry and material.

At plate boundaries the applied load causes plastic deformation of the surface asperities reducing interfacial voids. Bonding then continues by diffusion controlled mechanisms including grain boundary diffusion and creep. A strong diffusion bond is formed when grains grow across the boundary, with grains ideally tripling in size. Bonds strengths 85-95% that of the base metal are achievable with sufficient grain growth [9]. Diffusion bond strength is of great concern in designing PCHEs for thermal shock testing. The success or failure of diffusion bonding is primarily governed by three bonding variables, namely, the bonding temperature, the bonding pressure, and the holding time. Furthermore, the bonding surfaces should have a good surface finish and be clean and free from oxide films and adsorbed grease.

Simple alloys, such as 316 stainless steel, diffusion bond well, with strengths 85-95% that of the base metal. PCHEs bonded out of these simple alloys are also proven to take thermal shock and fatigue well. The 316 PCHE of Pra et al. [10] withstood 100 cycles of rapid heating to 510°C and cooling to 180°C. After all runs, helium leak testing of the fatigued PCHE didn't find any leaks.

High temperature alloys desired for use with the HTGR do not diffusion bond as easily. Stabilizing agents, such as Al and Ti in Inconel 617 and Nb in 347 stainless steel, form tenacious oxide layers that interfere with diffusion bonding [9]. These layers can be removed and replaced with an interlayer, but bond strength is a concern. To bond an IN617 PCHE specimen by diffusion, the Ohio State University was able to electrolytically plate a 2.5-µm-thick interlayer of pure nickel to the IN617 bonding surface. This layer eliminated the formation of oxide layers prior to diffusion bonding. A scanning electron micrograph of the diffusion bond is shown in Figure 10. Although allowing IN617 to be diffusion bonded, the nickel interlayer presented a weakened bond. The interlayer which inhibited grain growth was a weaker material, and brought many inclusions from the plating process into the diffusion bond. Tensile and creep tests found a bond with a ~30% reduction in ultimate tensile strength, with failures occurring at the nickel interlayer. [11]
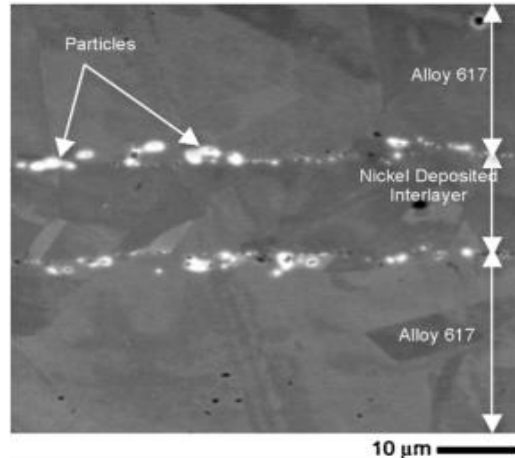
Fig. 10. SEM micrograph of diffusion bonded IN617 plates featuring pure Ni interlayer.
Second phase particle bound the Ni interlayer. [10]

Modeling Methodology

The geometry of the airfoil PCHE structure is modeled at three different scales, the local scale, the cross-section scale, and the full heat exchanger scale. Illustrations of the three scales are shown in Figure 11. The local scale included the structure immediately surrounding a single channel and can be generally modeled as a unit cell which can be repeated to build up the overall heat exchanger. The cross- section scale encompasses a segment of all heat exchanger's channels or plates including the walls and surrounding support structures. Obviously, modeling the cross-section scale is considerably more computationally intense than the local scale. Finally, the full heat exchanger scale looks at the entirety of the heat exchanger including the flow manifolds. It is the most complex and is often simplified with porous media properties drawn from the local and cross-section scales.
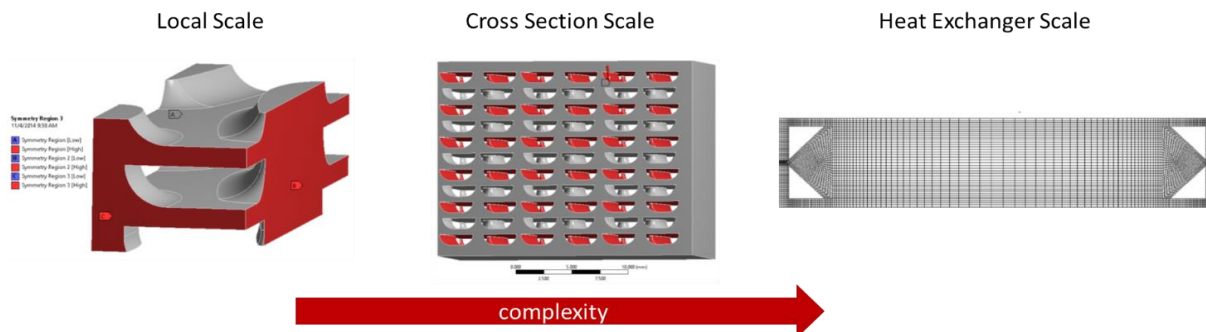
Fig. 11. Geometry scales of the PCHE models

Three degrees of increasing complexity can also be used to describe the elastic model, the plastic model, and the creep model, respectively. The elastic model is a simple linear stress-strain model with Young's Modulus of Elasticity as the slope of the stress-strain curve. However, this model is only valid up to the yield stress, at which point the plastic model must be used. The plastic model assumes the true stress-strain curve above the yield point is known. Figure 12 depicts the stress-strain relations used in model. The creep model is the most complex and must be built out of a set of plastic stress-strain models each from different length creep tests. The stress models available depend on the quality of material data available. Stress-strain data for 316 stainless steel can be found in the ASME Boiler and Pressure Vessel Code (BPVC) [12].
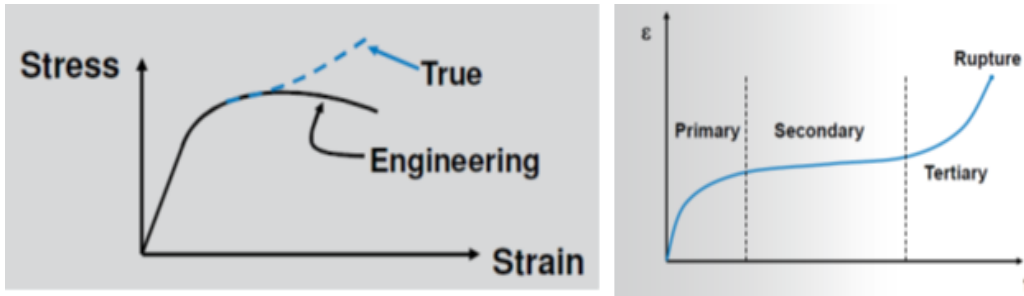
Fig. 12. Stress models used in the ANSYS solver, (left) linear elastic model and its extension into the plastic model, (right) full creep model

ANSYS Mechanical and ANSYS Workbench were used in the finite element analysis (FEA) of the airfoil PCHE system. In all models the geometry of interest is transformed into a mesh of tetragonal elements which is used by the ANSYS solver. The ANSYS solver is an iterative force-based solver. From the geometry and loading conditions, the forces on each element are resolved. With the forces set for each element of the geometric mesh, strain is varied and the process repeated until a solution converges. The ANSYS solver can handle all three stress models and calculates strain in the order of model complexity, from elastic, through plastic, to creep, as shown in Eq. 4 below.

$$\varepsilon = \varepsilon_{elastic} + \varepsilon_{plastic} + \varepsilon_{creep} \qquad [4]$$
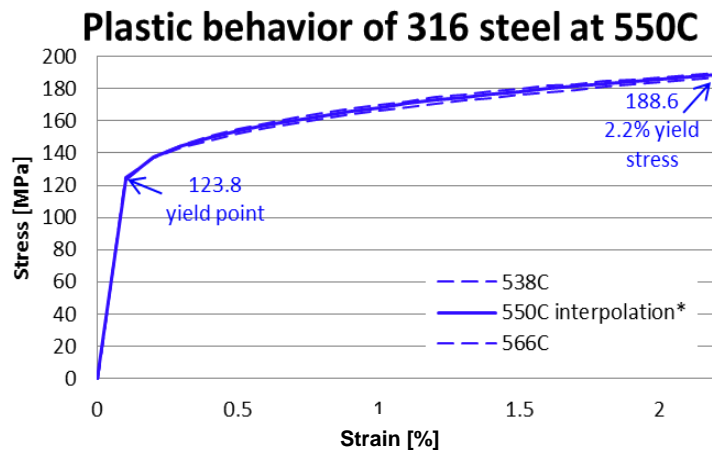
Fig. 13. Stress-strain data for 316 stainless steel at 550°C

Plastic and elastic properties of 316 stainless steel were obtained from the ASME BPVC [12]. Data was extracted from stress-strain charts in the BPVC's main pressure vessel section (Section III Division I). The charts show experimental stress-strain data at 15 different high temperatures ranging from 427°C to 816°C with creep tests of up to 34 years performed at all temperatures. Chart data was simplified to a 9 data point fit for each temperature's elastic stress-strain curve. Since BPVC data is only given for 15 discrete temperatures, data for intermediate temperatures was interpolated. For example, stress-strain data for 316 stainless steel at 550°C was interpolated from BPVC data for 538°C and 566°C as shown in Figure 13.

Elastic Model Results

Elastic models were the first developed because of their simplicity and usefulness in determining qualitative mechanical properties. The location of stress concentrations within the geometry and the effect of boundary conditions and supporting walls in a section are easily found. The results of the elastic models were useful in furthering of 316 stainless steel models.

Local scale elastic modeling highlighted the head and tail of the airfoil-fin as the area of concern for airfoil PCHE systems. The local scale is enforced by applying symmetry conditions to the six faces of the unit cell. In these models 20 MPa of pressurization in the airfoil channel created stress concentrations in excess of the yield point of 316 stainless steel (123.8 MPa at 550°C) [5]. Figure 14 shows the location of the tail side stress concentration in an elastic model. Here the lower airfoil channel is pressurized while the upper straight channels are not pressurized. Large curvature at the head and tail combine with the diffusion bond interface to create a high localized concentration of stress.

Increasing the coverage of airfoils in the section by decreasing the lateral spacing between airfoil columns brings the stress concentration down by distributing the 20 MPa within the channel over more tightly packed airfoils. Decreasing the curvature at the tail of the airfoil by rounding its profile also decreases the stress concentration, as the geometric concentration is more spread out. This can be seen in the plot of results shown at the right in Figure 14. Here the maximum stress at the concentration is compared to the airfoil coverage for various tail rounding. The embedded picture shows the four rounding profiles, with more rounding creating less curvature at the airfoil tail.
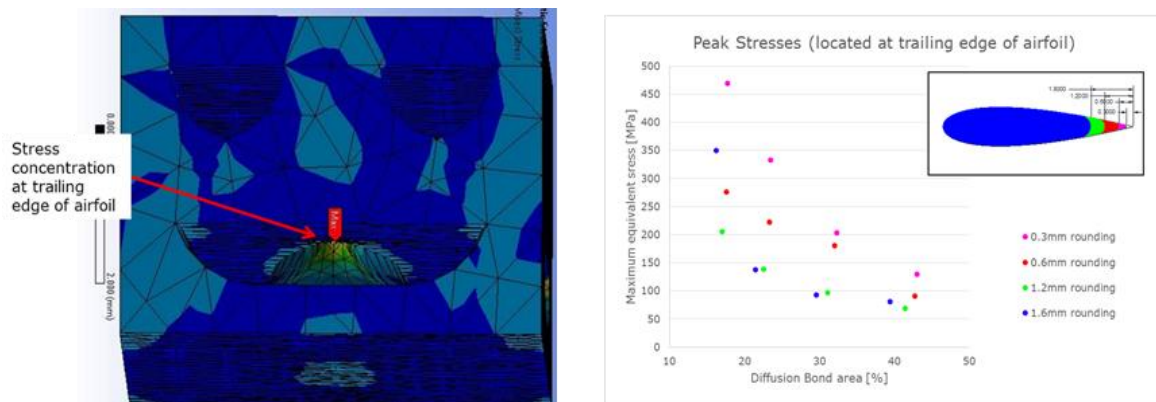
Fig. 14. (left) tail side stress concentration on a local scale model. The bottom channel is pressurized while the top channel is without pressure. (right) plot of local elastic model results for stress concentration at the airfoil tail for various channel coverage and rounding of the airfoil tail

Next, cross-section scale elastic modeling was used to show the effect of wall structures in the PCHE cross section and to determine the location of first failure in a section of PCHE. Since stress concentrations at the tail of the airfoil-fin were identified as the local stress concentration of interest in previous models, they were used in the evaluation of variation of stress states in a cross-sectional sample. The cross section of concern consists of 11 stacks of airfoil plates surrounded by exterior walls, as shown in Figure 15. The plates are 12 airfoil columns wide and feature the airfoil pattern shown in Figure 9.
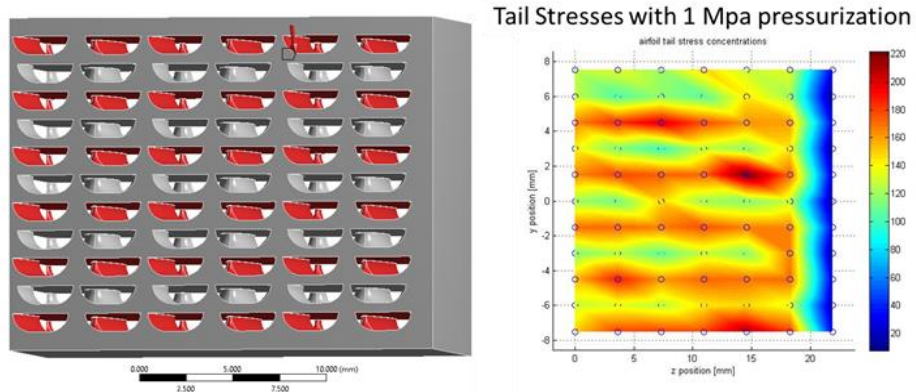
Fig. 15. (left) elastic cross-section model featuring 11 stacked airfoil channels and supporting PCHE walls. Red channels are pressured. Symmetry about left face is used to get a full cross section. (right) airfoil tail stress results for the elastic cross section model. Airfoils near wall have lower stress due to wall support. Pressurized channels have highest stresses.

Symmetry is used at the center of the cross section, the left face of Figure 15 being the centerline and symmetry of the cross section while the right face is the surrounding wall. In the model the cross section is pressured to 1 MPa at every other plate and the stress concentration is evaluated at each airfoil tail. A plot of the airfoil tail stresses over the cross section is shown on the right side of Figure 15 with circular points representing the location of each airfoil tail. The airfoil tails next to the PCHE wall, on the right side of the model, exhibit the least stress as they are substantially supported by the adjacent wall. This support diminishes quickly when moving away from the wall. It was found that all but the airfoils nearest to the wall see the impact of the wall's support and thus are stressed similarly. Higher stresses occurred in the pressurized channels than those without pressurization. This inter-channel stress difference can be seen in the horizontal striations of Figure 15.

Plastic Model Results

Plastic models were used to extend the simulation effort past that of previous elastic models. In PCHEs constructed of 316 stainless steel and other ductile metal the stress concentration seen in elastic models yields away. Plasticity at the stress concentration allows the stress to spread out within the yielding section. Yielding is allowable to some extent, as small features that contain stress concentrations make up a miniscule portion of the overall supporting structure. The airfoil PCHE structure should be able to withstand pressurization far above that which initiates the onset of yielding.

A local plastic model was developed to investigate the propagation of yielding in a singular airfoil-fin. The model is shown in Figure 16 and consists of a single air-foil fin under a tensile load. Tensile loading is the primary form of loading in the pressurized airfoil PCHE system. The model contains a geometric mesh with refinement of the mesh size at the diffusion bond interface and further refinement at the head and tail of the airfoil fin. The area of interest with respect to yielding is the diffusion bond interface, as it is the weakest part in the PCHE assembly and also the area of highest stress.
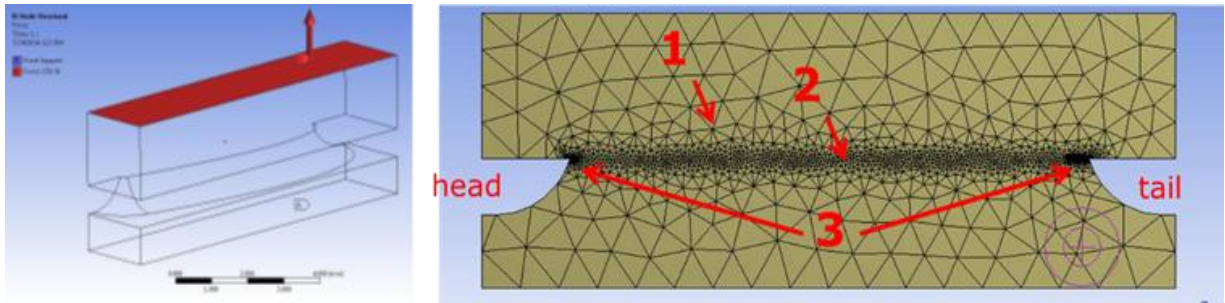
Fig. 16. Plastic model of airfoil in tension. (Left) tensile loading, (right) refinement of the model mesh with course mesh in channel was (1) refined mesh at the diffusion bond interface (2) and further refinement at the head and tail(3)

Solving the plastic airfoil-fin tensile model for various tensile loads shows the propagation of yielding in the airfoil. Figure 18 shows the distribution of stress along the diffusion bond interface with the areas of highest stress (in red) propagating through yielding from the head and tail of the airfoil. A 0.2mm thin area around the diffusion bond was analyzed to determine the extent of yielding. The percent of diffusion bond yielded was taken as the percent of this thin volume that was in excess of the 316 stainless steel yield stress of 123.8 MPa at 550°C. The airfoil can hold loads up to 1200 N at 550°C with the diffusion bond yielding no more than 20%. A plot of yielding with tensile load and a plot of yielding as a function of airfoil coverage at 20 MPa pressurization can be seen in Figure 19.
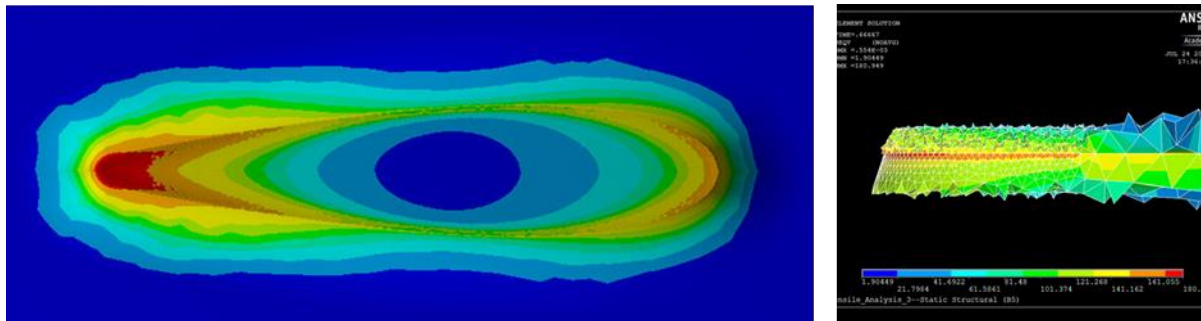
Fig. 18. Propagation of yielding at the diffusion bond interface. (left) yielding propagates from head and tail of airfoil diffusion bond, (right) close up of yielding at the tail of diffusion bond
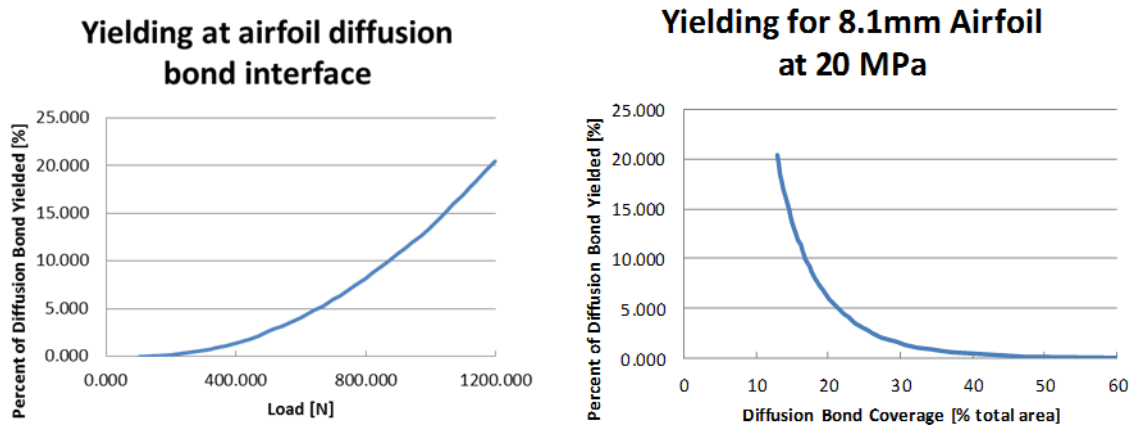
Fig. 19. Percent yield of the diffusion bond interface, (left) in terms of load on a single airfoil, (right) in terms of airfoil bond coverage with pressurization of 20 MPa

ASME BPVC Section VIII Compliance

The University of Wisconsin Madison has experience meeting American Society of Mechanical Engineering's (ASME) Boiler and Pressure Vessel Code (BPVC) requirements for PCHE channels through the mechanical finite element analysis (FEA) methods. These methods were used to verify the mechanical integrity of a PCHE produced by an industry partner. Although the results of the investigation cannot disclosed here, the experience and procedures created are readily applicable to the micro-channels being investigated.

Modeling of loading and fatigue in an industry partner's production heat exchanger was performed using numerical assessment as outlined in BPVC Section VIII Division 2 paragraph 5. In particular three of the four design-by-analysis requirements outlined in paragraph 5.1.1.2 were directly addressed through modeling: Protection Against Plastic Collapse, Protection Against Local Failure, and Protection Against Failure From Cyclic Loading. These requirements were addressed with the appropriate numerical models specified in paragraph 5.1. The BPVC procedures for modeling and analysis for each of the three requirements are outlined in
Table .

Table 2. ASME BPVC Design by Analysis Requirements

Protection Against Plastic Collapse	5.2.4 Elastic-Plastic Stress Analysis Method
" " Local Failure	5.3.3 Elastic-Plastic Analysis
" " Failure From Fatigue Loading	5.5.4 Fatigue Assessment (Elastic-Plastic Stress Analysis and Equivalent Strains)

The 316 stainless steel construction of the PCHE was modeled in accordance with ASME BPVC requirements for numerical analysis in BPVC VIII division 2 paragraph 5.1.2.4. The material model was built from the appropriate BPVC specified physical properties, strength parameters, stress-strain curves, and cyclic-stress-strain curves for 316 stainless steel. Non-linear material definition files were created for the ANSYS APDL FEA software package that was used. Non-linear material definitions were used so that localized yielding within micro-channel features could be accounted for.

To model both thermal and mechanical loads, combined conduction and mechanical FEA models were solved. Steady-state and transient simulations of conduction between PCHE channels were made. Temperature distributions from the conduction models were used as thermal strain input to mechanical models. Applied to each time step in the transient conduction model, mechanical modeling was used to determine the time varying stress distribution within the heat exchanger.

NONDESTRUCTIVE ANALYSIS

Nondestructive evaluation is an important technique for ensuring the integrity of nuclear-grade equipment. As part of federal regulations, systems which contain the primary reactor coolant (Class 1 components) are thoroughly inspected during scheduled and some unscheduled shutdowns for excessive wear or damage. To reduce the time and cost associated with these tasks, technicians need to be able to quickly identify if and where a component has failed. Section XI of the BPVC addresses non-destructive evaluation techniques of nuclear-grade equipment and is closely related to Section III which addresses construction of these components. In the extensively-used shell and tube heat exchangers, visual inspection, ultrasonic imaging, and gas leak detection provide a relatively quick and easy method to determine whether the unit meets its safety criteria. As previously mentioned, because the Electric Power Research Institute (EPRI) has extensive experience with these methods, it has elected to lead an effort to identify and review applicable NDE techniques as a part of this code case development project. Unfortunately, PCHEs and most other compact heat exchangers have channels which are far too small to allow for visual inspection and dense enough to severely limit ultrasonic imaging capability of the internal geometry. Methods to enhance the utility of these existing techniques such as view port and header removal for mid-life inspection are being reviewed in addition to the radiography techniques discussed below.

X-Ray Tomography

In 2017, CompRex, LLC provided a series of PCHE to the University of Wisconsin for burst testing by pressurizing using room temperature water until the unit failed. These PCHEs all withstood pressures above 15,000 psi before internal separation of the plates occurred. Three units which closely resemble those to be tested under prototypic conditions in this project all exhibited an internal failure while the outer boundary of the PCHE remained intact despite significant deformation. Furthermore, the internal separation did not result in penetration of the fluid boundary and in most cases external deformation was minimal. During these tests, a steep drop in pressure due to plastic deformation (volume expansion) suggested some type of failure had occurred. However, determining the nature of this failure requires visualization of the internal structure. To visualize the failure without cutting or physically altering the block, x-ray computed tomography (CT) was used. Computed tomography creates a 3-D rendition of an object by rotating it within a beam of high-energy x-rays. A scintillation detector creates images of the object based on the number of x-rays that are absorbed or scattered by the object of interest. By rotating the object at an interval related to the "capture rate" of the detector, a three-dimensional collection of points, known as a "point cloud", is obtained. Using an industrial reconstruction software, the point cloud is transformed into a digital geometry shown in Figure 20.
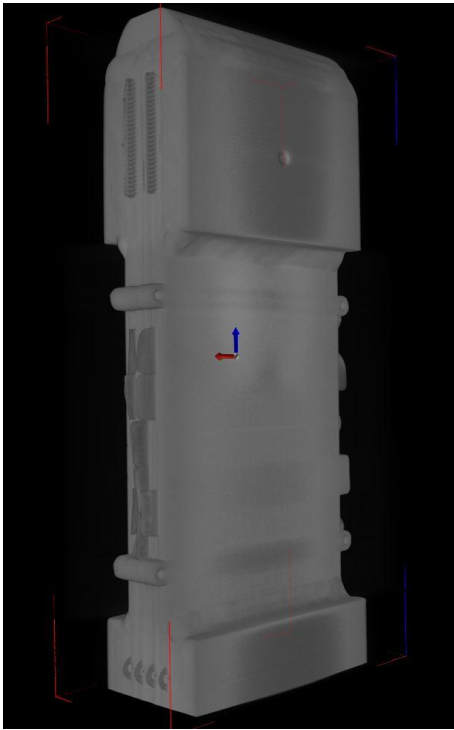
Fig. 20. 3-D reconstruction of ShimRex® PCHE
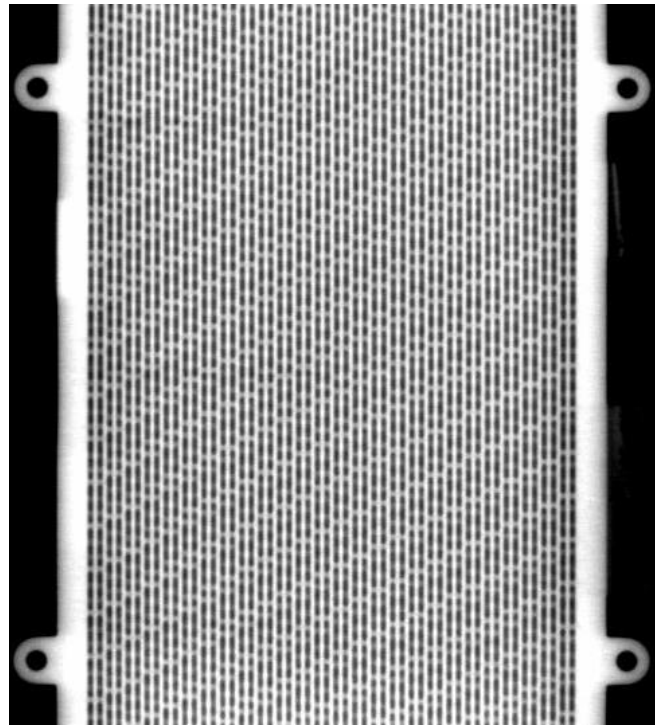
Fig. 21. Top view of ShimRex® PCHE

The reconstruction software allows the user to view any location in the object and identify troublesome features less than 100 microns in size. X-ray imaging systems using 450 kV and 9 MV excitation voltages were used to take a CT scan of one of the failed PCHEs. The higher excitation voltage of the 9 MV system produced higher energy x-rays which can penetrate thicker pieces of steel. As a result, the contrast and resolution of the 9 MV images were noticeably better. Figure 21 shows an image of a single ShimRex® plate obtained from the 9 MV reconstruction in Figure 20. This method allows the analyst to scroll through the PCHE and inspect each plate and the alignment between plates. Slight misalignment of the plates has occurred during the diffusion bonding process. When channels are small, even miniscule misalignment can produce a significant stress concentration and possibly lead to premature failure. The clarity of both the 450 kV and 9 MV images have shown great potential to identify these features in these lab-scale PCHE. This work will help to define the allowable limits of this plate-slip phenomenon.

A portion of this project's funding has been used to purchase a 450 kV x-ray system, which will

reside at the University of Wisconsin. This system should be installed in time for CT scans of the PCHE to be tested in Task 3. After a defined testing interval(s), the PCHE will be returned to UW for additional scanning. Comparison of these image sets will determine the utility of CT for identifying corrosion and/or clogging effects within channels. Scans will also be taken after thermal shock-induced failure or rupture testing to identify failure mechanisms at the end of the testing period.

While the x-ray technique works well for the relatively small PCHE (24" x 6" x 2") supplied by CompRex, scaling up of this method presents a few challenges. First, as the PCHE becomes thicker and wider, the x-ray energy required to penetrate it increases and the contrast of the image decreases. Secondly, only a few facilities in the world have systems large enough to image objects that extend beyond a cubic yard. Finally, x-ray imaging requires radiation shielding that may pose logistical challenges if the PCHE is not within the containment structure. Due to these reasons CT inspection of commercial-scale PCHE is likely not a viable means of scheduled inspection, but it is a valuable tool developing the operational limits of PCHE and may be useful for inspection of cores immediately after diffusion bonding.

Neutron radiography

Another evolving method of NDE is neutron radiography, which uses neutrons produced by subcritical assemblies or nuclear reactors to penetrate dense objects. The challenge of producing a high population of neutrons has constrained the capabilities of neutron imaging compared to x-ray radiography. A major obstacle is finding a neutron source with a sufficient flux for imaging on a reasonable time-scale. Phoenix LLC, founded by a University of Wisconsin doctoral graduate, specializes in neutron imaging technologies. Their latest system is capable of fluxes up to 10^4 n/cm^2·s which can image most objects in a few hours. Neutrons created by a D-T reaction are funneled towards a confined sample area, pass through the PCHE and strike a special film which is processed to yield the radiographic image shown in Figure 22.
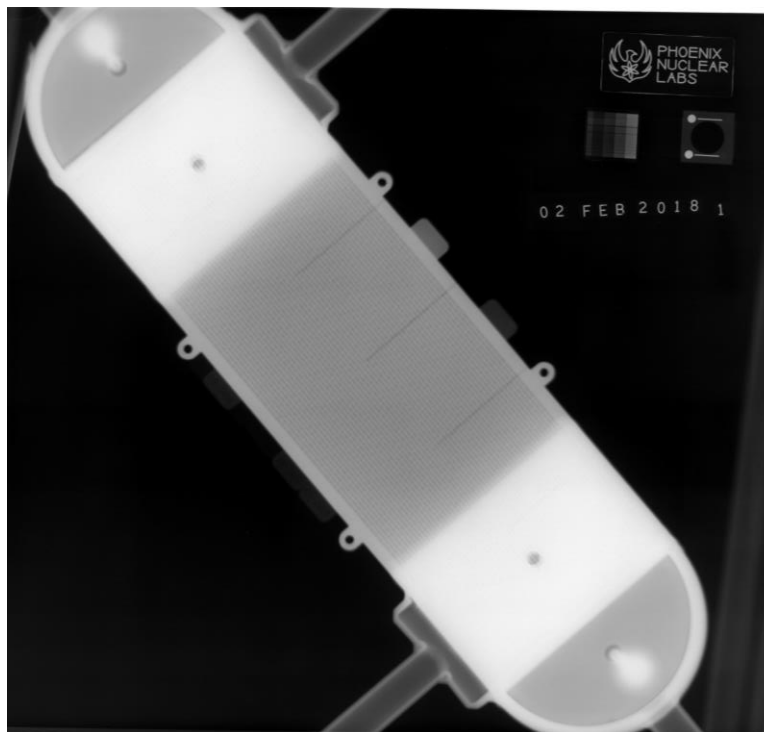
Fig. 22. Neutron radiograph of PCHE with attached headers

Similar film methods were used for x-ray imaging before high-speed scintillation detectors hit the market. Unfortunately, high-resolution neutron scintillation detectors are not commercially-available at this time. Still neutron radiography has its benefits. Firstly, neutrons easily pass through metals unlike x-rays which are scattered or absorbed by the electrons of high-Z elements such as iron, nickel, and chromium. Secondly, if the channels of a PCHE are flooded with a penetrating hydrocarbon-based liquid (such as WD-40) and then drained, cracks still containing the penetrant will show up dark on the image due to neutron

absorption. The scan shown in Figure 22 has a resolution approaching 100 microns over an acquisition period of 5 hours. This resolution and scan time is surprisingly similar to the results of the 450kV x-ray system. The ShimRex PCHE imaged using x-ray CT has now been sent to Phoenix for neutron imaging shortly after a system upgrade. These images will provide an excellent visual comparison of the two methods and hopefully provide additional insight into crack formation and propagation within the PCHE core. At this time, the PCHE supplied by CompRex are approaching the size limits of Phoenix's system. Thus, the project leads are working with Oak Ridge National Laboratories to use the Spallation Neutron Source for additional imaging and computed tomography of the PCHEs to be tested in the coming months. This facility produces neutron fluxes that are three orders or magnitude greater than Phoenix's facility and imaging space can easily accommodate the PCHE discussed here, but costs may be significantly higher.

DESTRUCTIVE TESTING

The integrity of the diffusion bond in printed-circuit heat exchangers enables them to withstand pressures more than 10 times their design pressure. In fact, Vacuum Process Engineering (VPE) has performed tensile tests of SS316 diffusion bonds which have strengths within the range of the base material. As a result, the weak spot of these prototypic PCHE is actually within the headers or near the welds that attach the headers to the core. In some ways this may simplify code qualification efforts if the primary failure mechanism is related to the headers. Existing code sections which address header sizing and attachment may be used for PCHE qualification. However, the failure mechanisms of the PCHE core itself need to be identified. CompRex intentionally designed their burst-test PCHEs with ½" inch thick plates welded to ends of the core for reinforcement of the header attachment areas, as shown in Figure 23 below. These reinforcements also strengthen areas where one of the flow streams makes a 90° turn to enter/exit through the sides. The entrances of the unpressurized fluid passages can be seen on the left end of Figure 23.

Fig. 23. PCHE with reinforced header region

A special pressurization system was constructed at the University of Wisconsin to test four ShimRex© geometries for comparison with estimated rupture pressures. A screw pump and high-pressure lines rated to 60,000 psi routed water to the PCHE. Signals from a piezoelectric pressure transducer and strain gauges were read by a LabVIEW program. Since strain gauges only provide information about a localized region, a digital image correlation strain-measurement technique was also used. Using a speckle pattern spray-painted on the PCHE's exterior and a pair of digital cameras, the motion of the speckles shown in Figure 24 could be tracked in real time. Using an industry software, the displacement is determined by measuring motion of the speckles between pictures. Since the cameras are located ~15° off the normal vector of the surface, displacement towards the camera (out-of-plane) could be measured as well. The calculated displacement components could then be used to calculate the strain vector components and the results can be plotted as shown in Figure 25. The precision of this method is on the order of strain gauge measurements, with the obvious advantage of measuring the entire surface. Digital image correlation techniques are being investigated by Sandia National Laboratories as a means of non-destructive evaluation for this project. In theory, a speckle pattern resilient to high temperatures could be painted on the surface of commercial scale PCHE to measure strains during transient tests immediately after construction or during scheduled inspection periods by temporarily removing the insulation.
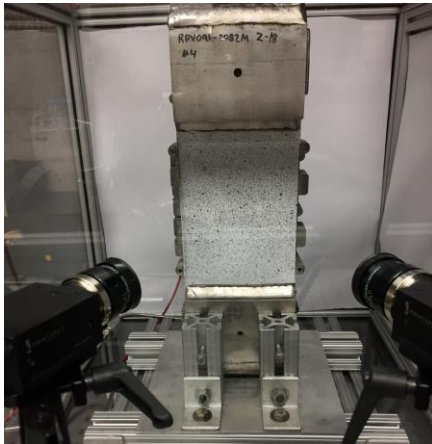
Fig. 24. Cameras imaging speckle pattern
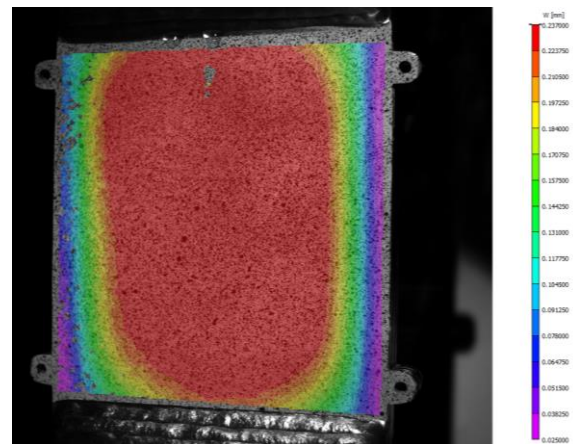
Fig. 25. Z-displacement contour map

CompRex® has permitted the author to include results from one of the pressure tested PCHEs that were imaged using x-ray CT. This unit, shown in Figure 24, consists of two atmospheric channel sets above and below a pressurized channel set, as shown in Figure 26. For reference, plates are stacked to build up the vertical dimension of the PCHE in Figure 15. The adjacent pressure trace in Figure 27 provides a timeline for the pressurization of this sample. At 250 seconds, the low pressure pump raised the system pressure to a level equating to 14% of the failure pressure. The low-pressure pump was isolated at this time and pressurization resumed by turning in the screw of the high-pressure screw pump. At approximately 500 seconds, the PCHE was isolated so the screw pump could be refilled and the lines upstream of the isolation valve could be brought back to the appropriate pressure. At approximately 650 seconds, pressurization resumed. The screw pump was turned in at the same speed as during the first stroke but the rate of pressure increase slumped as yielding occurred. Shortly after, failure occurred in a localized area in the middle of the central channel, as seen in Figure 26 and 28.
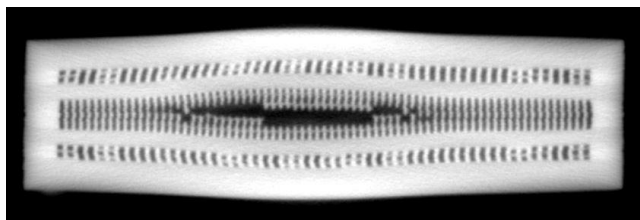
Fig. 26. End view of ruptured ShimRex® PCHE
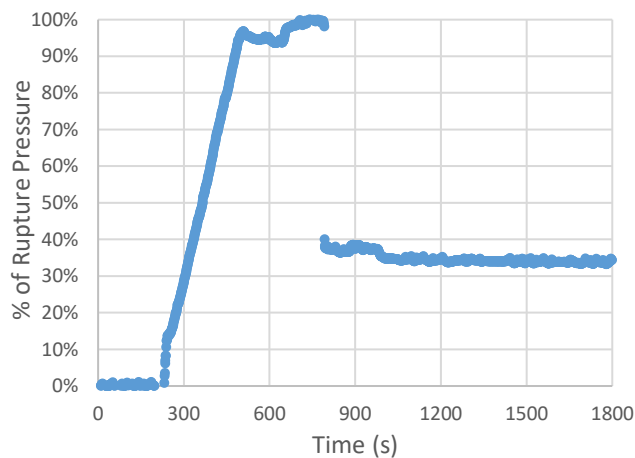
Fig. 27. Pressure trace during burst test of a ShimRex® PCHE
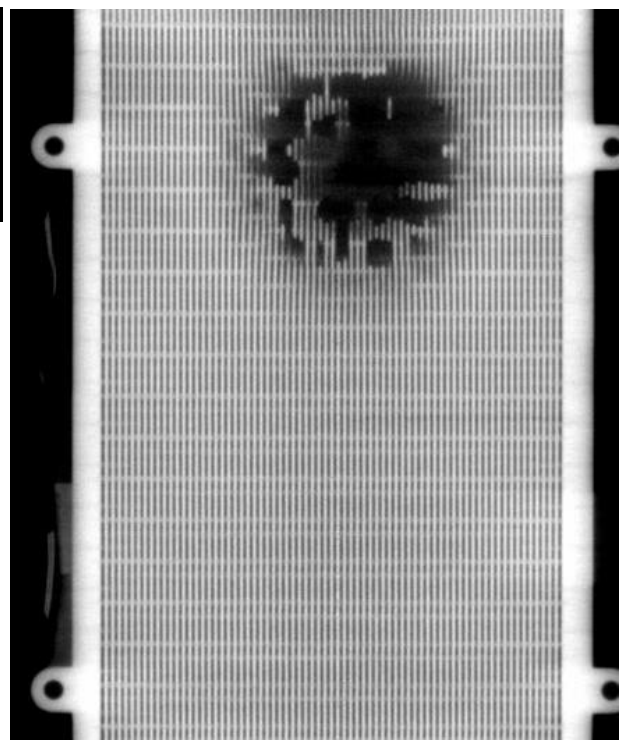
Fig. 28. Delamination observed after burst test

Figure 28 shows one of the ShimRex plates in the ruptured PCHE. The dark area shows where some of the channel "grid" has been torn away from the original plate and remains diffusion bonded to the adjacent plate as seen in Figure 26. As plate separation occurred, the total volume in the central channel set increased and the pressure dropped to approximately 35% of rupture pressure. This PCHE was isolated from the pump and left at pressure overnight. 20 hours after the failure was observed, the PCHE remained around 30% of rupture pressure. This is a testament to the strength the PCHEs and their ability to contain a fluid at high pressures even after an internal failure has occurred. These tests were a great learning opportunity for the IRP researchers. The availability of these results early in the project have helped to identify the types of failures to expect. The magnitude of the pressure required to separate the internal structure reinforces the idea that the headers and attachment (weld) zones are the primary failure mechanism. Further investigation will identify when this is not true and if designs that do not exhibit this behavior should be avoided for simplify certification efforts.

CONCLUSION

This paper summarizes the Integrated Research Project to develop a nuclear code case for printed-circuit heat exchangers. This project will utilize an iterative process to improve testing procedures and to develop an ASME BPVC code case through collaboration of multiple research institutions. The five task groups: code development, material properties testing, prototypic PCHE testing, non-destructive, and destructive evaluation will work together using a feedback mechanism to make meaningful progress towards certification. MPR Associates, a firm with experience in Boiler and Pressure Vessel application and development, will modify existing compact heat exchanger codes from Section VIII to attempt fulfillment of the Section III criteria. Measured material properties and experimental PCHE data from collaborative university research will help to fill technical holes in the Section III code case draft. Additionally, the non-destructive and destructive evaluation components of the project seek to identify new inspection methods and to identify failure modes through modeling and testing. The results of these studies will be crucial to the Section III and Section XI developments and to continued application of printed-circuit heat exchangers in the energy industry.

Code case development will be supported through experimental and modeling methods. Experimental heat exchangers will use supercritical CO_2 in the Alloy 800H and SS316H PCHE set. A new facility at the University of Wisconsin will be the third operational loop on-site capable of testing heat exchangers and regenerators over a wide range of pressures and mass flow rates. Testing strategies will be honed to evaluate systems linking supercritical CO_2 to a series of advanced nuclear coolants such as fluoride salts, sodium, and helium. Additionally, upcoming non-destructive inspection and burst tests will build confidence in the herringbone and ShimRex® geometries while developing quality assurance techniques that may be useful to the PCHE and by association the supercritical CO_2 industry. Experimental efforts will be guided and supplemented by modeling. Plasticity and creep models will be used to predict failure in ratcheting, pure creep, and thermal shock tests. Creep life of PCHEs beyond the 1000 hours that can be experimentally be tested will be determined through modeling.

Experimentation, inspection, and modeling will build support for the certification of compact heat exchangers for nuclear service. This work will culminate in an ASME BPVC section III code case for compact heat exchangers. In addition, exposure to new coolants and state-of-the-art inspection technologies will further inform PCHE design for next-gen nuclear applications.

ACRONYMS & NOMENCLATURE

ASME = American Society of Mechanical Engineers
BPVC = Boiler and Pressure Vessel Code
CHE = compact heat exchanger
CT = computed tomography
FEA = finite element analysis
FHR = fluoride salt-cooled high-temperature reactor
LWR = light water reactor
PCHE = printed-circuit heat exchanger
sCO_2 = supercritical carbon dioxide

ΔP = pressure change across PCHE [Pa]
f = Darcy's friction factor [-]
L = Channel set length [m]
D_h = hydraulic diameter of channel set [m]
ρ = fluid density [kg/m^3]
v = bulk fluid velocity [m/s^2]
μ = fluid dynamic viscosity [Pa-s]
$\dot{m}$ = mass flow rate through channel set [kg/s]
A_c= cross-sectional area of channel set [m^2]
Re = Reynolds Number [-]
j = Chilton-Colburn heat transfer coefficient
h = local heat transfer coefficient [W/m^2-K]
U= overall heat transfer coefficient [W/m^2-K]
Pr = Prandtl number [-]
C_p= fluid specific heat capacity [J/kg-K]
$A_s = A$ = heat transfer surface area [m^2]

REFERENCES

[1] Gen IV International Forum, *Technology Roadmap Update for Generation IV Nuclear Energy Systems*. Brussels, Belgium, Jan. 2014.
[2] X. Li, R. L. Pierres, S.J. Dewson, "Heat Exchangers for the Next Generation of Nuclear Reactors", Proceedings of ICAPP '06 Reno, NV USA, June 4-8, 2006 Paper 6105
[3] A. Kruizenga, D. Fleming, M. Carlson, and M. Anstey, "Supercritical CO2 Heat Exchanger Fouling," in The 4th International Symposium - Supercritical CO2 Power Cycles, Pittsburgh, Pennsylvania, 2014, pp. 1–9.
[4] Luna Innovations Incorporated, "Optical distributed sensor interrogator," Model ODiSI-B datasheet, Aug. 2014
[5] J. Hesselgreaves, *Compact Heat Exchangers: Selection, Design, and Operation*, Second Edition. Elsevier Publishing, 2017.
[6] J. Nestell, T. L. Sham, "ASME Code Considerations for the Compact Heat Exchanger", Oak Ridge National Laboratory, ORNL/TM-2015/401. August 2015.
[7] T. Habisreuther, T. Elsmann, A. Graf, M. A. Schmidt, "High-Temperature Strain Sensing Using Sapphire Fibers With Inscribed First-Order Bragg Gratings," *IEEE Photonics Journal*, vol. 8, no. 3, June 2016.
[8] M. Carlson, "Measurement and Analysis of the Thermal and Hydraulic Performance of Several Printed Circuit Heat Exchanger Channel Geometries," M.S. Thesis, University of Wisconsin Madison, (2012).
[9] Personal conversation with Norm Hubele of Refrac Systems, June 9, 2014.
[10] F. Pra, P. Tochon, C. Mauget, J. Fokkens, S. Willemsen, "Promising Designs Of Compact Heat Exchangers For Modular HTRs Using The Brayton Cycle," Nuclear Engineering and Design, 238, 11, 3160, (2008).
[11] S. Mylavarapu, X. Sun, R. Christensen, R. Unocic, R. Glosup, M. Patterson, "Fabrication And Design Aspects Of High-Temperature Compact Diffusion Bonded Heat Exchangers," Nuclear Engineering and Design, 249, 49-56, 49, (2014).
[12] ASME BPV Code, Section III Division 1 - NH, (2013)
[13] A. M. Kruizenga, "Heat Transfer and Pressure Drop Measurements in Prototypic Heat Exchangers for the Supercritical Carbon Dioxide Brayton Power Cycles," Madison, 2010.

ACKNOWLEDGEMENTS